Transparent conductive organic–inorganic hybrid composites based on Ag nanowires

Katharina Lang[1] · Matthias Klein[1] · Gerhard Domann[1] · Peer Löbmann [ID][1]

Abstract

Silver nanowires (AgNW) were incorporated into different organic–inorganic hybrids and a silicone composition that served as a reference. Spin coating yielded transparent conductive films, their respective nanowire distribution, thermal activation, and visual transparency were characterized. The percolation threshold of the films scales with the individual average AgNW length. Substantial conductivity was maintained throughout mechanical stretching up to 30%. Microstructured organic–inorganic hybrid composite films were obtained by UV lithography.

Graphical Abstract

Composites of hybrid inorganic–organic polymer resins with silver nanowires can be microstructured by UV lithography. Such films retain electrical conductivity even when stretched by 30%.
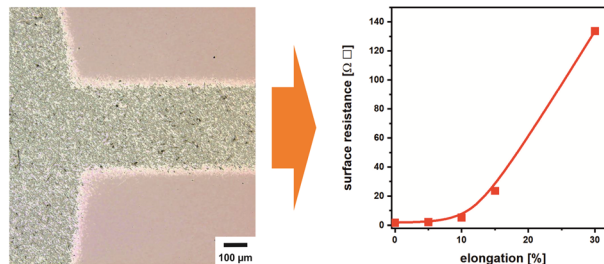
Highlights

- Silver nanowires (AgNWs) were introduced into organic-inorganic hybrid composites.
- Transparent conductive films were prepared based on this formulation.
- The resulting conductivity can well compete with sputtered transparent conductive oxides.
- The flexible films retain conductivity up to 30% stretching.
- Microstructured conducting paths were obtained by UV-lithography.

✉ Peer Löbmann
peer.loebmann@isc.fraunhofer.de

1 Fraunhofer-Institut für Silicatforschung, Neuenplatz 2, 97082 Würzburg, Germany

1 Introduction

Since their initial invention [1] the high aspect ratio of silver nanowires [2–4] was utilized for the fabrication of conductive films and structures [5]. As the early percolation into networks minimizes the material usage, transparent conductive films can be prepared using metallic silver [6, 7].

In contrast to transparent conductive oxides (TCOs) such as Indium Tin Oxide (ITO), Antimony Tin Oxide (ATO), or Aluminum-doped Zinc Oxide (AZO), silver nanowire networks are flexible [8, 9] and thus may withstand bending or even stretching [5, 10, 11]. Therefore, these materials are excellent candidates for flexible and stretchable transparent electronic devices [12–14] such as solar cells [15–17] and displays [18, 19].

In general, transparent films of sole AgNWs may be deposited in a thickness that only has to facilitate the overlap of single nanowires in order to establish a connective network. Such fragile microstructures, however, are extremely prone to mechanical damage [12, 20]. Therefore, protective layers are commonly applied [12, 21]. If these materials are insulating, the electric contacts to the functional AgNW film becomes a technical issue.

To overcome these problems silver nanowires may be incorporated into a polymer matrix system. Doing so the interconnectivity of the AgNWs will be handicapped. The use of such a composite, therefore, will always imply a tradeoff between electric conductivity, optical transparency, and mechanical performance.

Apart from single reports of Kim et al. [22, 23] silicones are primarily described as matrix materials for AgNW composites [12, 21, 24]. As technically mature materials, silicones are available in a broad range of mechanical properties at low cost. For electronic applications, however, the fabrication of elaborate microstructures by, e.g., UV lithography is required. In this respect, standard silicones only offer limited options [25]. Therefore, alternative matrix materials that can be laterally structured have to be considered.

Transparent organic–inorganic hybrids can fulfill these requirements: they consist of inorganic domains that are formed by hydrolysis and condensation reactions which may subsequently be connected by the organic polymerization of alkoxysilane sidechains [26]. If this organic reaction is induced by local irradiation and the uncured film regions are removed by a washing step, lateral microstructures are formed. The remaining pathways can offer a chemical and thermal stability similar to silicones due to their inorganic–organic nanostructure. Numerous optical and electrical applications have been realized by UV lithography [27] or laser processing [28] of organic–inorganic hybrids even on an industrial level.

To our knowledge, the compatibility of any organic–inorganic hybrid with AgNWs has not yet been demonstrated. For that purpose, as a first feasibility study we chose a polar and a nonpolar organic–inorganic hybrid for the preparation of two silver nanowire composites. A commercial silicone formulation was used to serve as a reference material.

2 Experimental procedure

2.1 Preparation of AgNWs

Polyvinylpyrrolidone (PVP) (M_w~55,000), silver nitrate (≥99%), sodium chloride (≥99%), ethylene glycol (EG) (99.8%), and Iron(III) nitrate (≥98%) were purchased from Sigma Aldrich, ethanol (99.8%, denatured with 1% methyl ethyl ketone) was purchased from CSC Jäklechemie. All chemicals were used as received without further purification.

The silver nanowires were synthesized by a modified polyol process developed by Sun et al. [29]. For this purpose 5.31 g PVP (M_W ~ 55,000, 0.097 mmol) was dissolved in 115.19 g EG by an ultrasonic bath and preheated to 140 °C. After reaching the requested temperature, 865 µl of a 0.22 mol/l NaCl-solution (0.19 mmol in EG) as well as 240 µl of a 0.2 mmol/l $Fe(NO_3)_3 \cdot 9H_2O$ (0.048 µmol in EG) were added to the hot solution and stirred for 5 min at 100 rpm. A previously prepared $AgNO_3$ solution (1.09 g in 28.82 g EG, 6.42 mmol, ultrasonic bath) was added dropwise while protecting from light in order to avoid photosensitive reactions. The mixture was stirred at about 140 °C for 90 min and cooled down to room temperature to add 50 ml ethanol.

The obtained suspension was centrifuged once for 15 min at 2000 rpm and after that several times for 10 min at 1500 rpm. Between every centrifugation step, the sediments were dispersed with 10 ml ethanol. Finally, all of the sediments were rejoined and transferred to a volumetric flask to determine the mass of the obtained silver nanowires.

Even if the conditions were kept constant, different syntheses resulted in different mean lengths of AgNWs. The investigation of the mean length of the nanowires was carried out by defining the reference distance in pixels (ImageJ) by means of laser scanning microscope images. On this occasion, the known distance of the inserted scale was set and determined as the standard. After marking all the single wires under sufficient magnification it was possible to compare them with the standard and to average them. At least, the data were used for numerical data analysis. Eighty percent of the syntheses resulted in average lengths between 10 and 20 µm. For the preparation of composites three batches with average AgNW lengths of 7, 12, and 140 µm were chosen.

2.2 Synthesis of matrix materials

The polar organic–inorganic hybrid was synthesized based on the EU patent EP 0 451 709 B1 [30].

Therefore, 0.05 mol 3-(triethoxysilyl)propyl isocyanate and 0.0025 mol dibutyltin dilaurate were added dropwise to 0.05 mol of the acrylate 1,4-butanediylbis[oxy(2-hydroxy-3,1-propanediyl)] diacrylate under moisture-free

atmosphere. After 1 h, the reaction is complete and a slightly yellow solution is obtained. For hardening Ciba® Irgacure® 500/369 functioning as a UV-hardener is used.

The synthesis of the nonpolar organic–inorganic hybrid is carried out by mixing 0.038 mol vinyl-trimethoxysilane, 0.4 mol vinylmethyldimethoxysilane, 0.5 mol diphenyldimethoxysilane, and 0.313 mol 3-methacryloxypropylmethyldimethoxysilane or 2-(3,4-epoxycyclohexyl)ethyltrimethoxysilane. As suitable catalyst 1.2 mol dil. HCl is added to the reaction mixture and stirred for 24 h at a temperature of 80 °C. The obtained solution is diluted with 7.6 mol of ethyl acetate and subsequently washed five times with 300 ml distilled water. All volatile components are removed within 20 h from the reaction mixture by rotational evaporation with a maximum bath temperature of 40 °C. Finally 23 wt% bis-[(dimethylsilyl)phenyl]ether as a crosslinking terminated SiH-reagent and 1 wt% of a diluted platinum-divinyltetramethyldisiloxane complex in xylene is added to the colorless resin to ensure hydrosilylation.

The silicone formulation contains 0.002 mol Mod 705, 0.0062 mol VQM 906, 0.0061 mol CL120 (Evonik Industries). The commercial silicone components were used as received without further purification and mixed together by a speed mixer. The curing step is processed by 0.1 wt% of a platinum catalyst that crosslinks the addition-curing silicone at room temperature.

2.3 Preparation of composites

We chose polar and nonpolar organic–inorganic hybrid/AgNW and silicone/AgNW composites by preparing a simple composite solution for application and characterization. Therefore, the as-prepared matrix system was diluted 1:10 with ethyl acetate or ethanol and mixed with the desired amount of an as-prepared ethanolic NW suspension. The specific volume fraction in a cured composite film depends on the concentration of the NW component and the solid-state densities of the used resins. It was also assumed that the mass of the AgNWs was evenly distributed over the whole film after spin coating. Consequently, the volume percentage of silver nanowires in the film could be calculated via $(m_{Ag}/\rho_{Ag})/[(m_{resin}/\rho_{resin}) + (m_{Ag}/\rho_{Ag})]$.

2.4 Film deposition and handling

For film deposition, the prepared suspensions were applied on a glass substrate or on an elastomeric substrate for mechanical measurements and spun with 3500 rpm over 20 s. The thickness is controllable by varying the rotational speed from 300 to 5000 rpm. After that, the sample was stored and dried for several minutes under ambient conditions before curing. The polar organic–inorganic hybrid material was UV cured with two mercury-vapor lamps (6 J/cm^2) and then tempered at 250 °C for 2 h. The nonpolar organic–inorganic hybrid material was heated up to 240 °C with a heating rate of 5 °C/min and hold at this temperature for 2 h. The same procedure was realized with a temperature of 230 °C for the silicone.

The samples for mechanical investigation were secured in the vice and stretched up step by step to more than 30% with subsequent releasing to the initial state. While stretching and releasing the electrical resistance was measured on the surface by an electrical four-point probe measurement setup.

For UV-patterning the nonpolar organic–inorganic hybrid was mixed with a UV starter (Ciba® Irgacure® 369 for acrylates, CYRACURE™ UVI-6974 for epoxide resins) and spin coated on a substrate (see above). After a first thermal treatment ("pre-bake") at 100 °C for 1 min, which is intended to limit the flowability of the material but not to affect its solubility in organic solvents, the stiffened conductive structures are produced by UV exposure (mask aligner MA6; 20 mW/cm^2) through a mask. After a further thermal step ("post-exposure bake") at 100 °C for 1 min the development takes place by removing the non-UV-exposed areas of the composite with the aid of a solvent (e.g., isopropanol). Finally, the remaining film was tempered in air atmosphere and residual Ag nanowires on the surface were removed mechanically (tape) or by means of an etchant (dil. HCl/HNO$_3$-solution or H$_2$O$_2$).

2.5 Characterization

The wetting behavior at any point on a solid surface was determined by a drop shape analysis system (A.KRÜSS Optronic GmbH) which is used flexibly for the precise measurement of contact angle and surface free energy by the sessile drop method.

The surface conductivity was measured at room temperature with a four-point probe on a 3458 A multimeter from Hewlett–Packard. For this purpose, the probe head was placed at five different positions on the surface to receive an average of all the measurements. As only the system getting the normal resistivity one has to consider to multiply the values by $\pi/\ln2$ to obtain the surface resistivity R_S [$\Omega \square$]. The specific conductivity σ is $1/(R_S \cdot d)$ with the film thickness d and the specific resistivity is $R_S \cdot d$.

The transmission measurement was performed by a Shimadzu UV3100. Technical glass such as borosilicate float glass (SCHOTT BOROFLOAT®) serves as substrate/reference. The wavelength range was set from 300 to 1700 nm. Including the Lambert–Beer law it was possible to calculate the values for transmission at the same thickness.
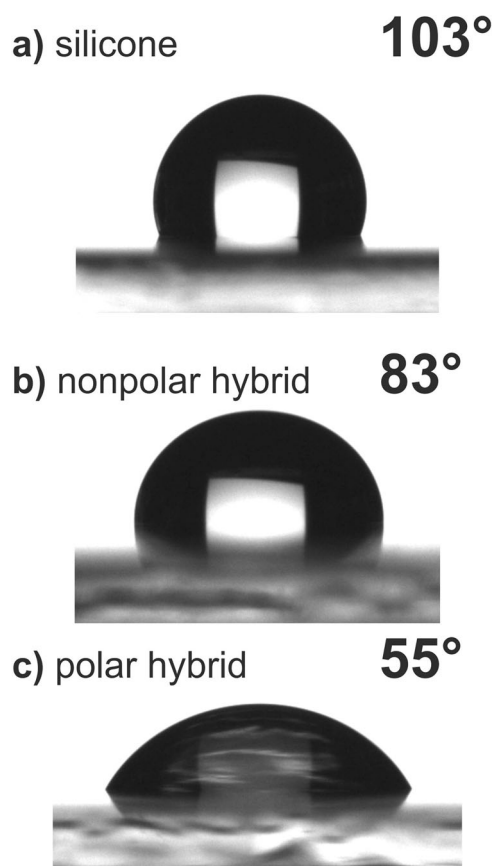
a) silicone   **103°**

b) nonpolar hybrid   **83°**

c) polar hybrid   **55°**

Fig. 1 Photographic image of water drops on a silicone film (**a**), a nonpolar hybrid (**b**), and a polar hybrid (**c**) along with the respective contact angles

A Keyence 3D-Laser scanning microscope VK-X100K/X200K was used for imaging. The optical and the laser image were combined by the instrument's software. The mean length of the AgNWs was determined by image analysis using the software ImageJ. During the examination of the composites, five image sections each were randomly selected and examined. No systematic differences in homogeneity were found, which is why a representative image was chosen.

3 Results and discussion

Since the polarity of the selected organic–inorganic hybrids was expected to have a critical impact on the dispersibility of silver nanowires, contact angles with water were measured. In Fig. 1 the results for two organic–inorganic hybrid compositions are shown in comparison to a standard silicone film that served as a reference. It can be seen that both systems show lower contact angles to water than the silicone film. As with 83° and 55° the two organic–inorganic hybrids show a significant difference in polarity, they subsequently will be referred to as "nonpolar hybrid" and "polar hybrid".

In the current literature, silicones are the polymers mostly used for the preparation of AgNW composites [31–33]. Due to the synthesis conditions, highly polar PVP molecules are adsorbed to the surface of standard silver nanowires [34]. The two organic–inorganic hybrids under investigation here thus presumably will have an even better compatibility to the AgNWs than silicones.

AgNW batches with average lengths of 7, 12, and 140 μm were used to prepare composites with the organic–inorganic hybrids and the silicone formulation. In order to check for a homogeneous nanowire distribution films were prepared and characterized by laser scanning microscopy (LSM). For these preliminary investigations a concentration of 3 vol% AgNWs was chosen, the results are summarized in Fig. 2. Up to lengths of 12 μm no nanowire agglomeration is detected for any of the matrix systems. Even though both organic–inorganic hybrids have higher polarities, the silver nanowires are also evenly distributed in the silicone. A complete percolation even for short lengths is visually suggested here. It has to be noted, though, that intersected nanowires may be separated by matrix material in the depth of the films. Therefore, electrical measurements are required to test the connectivity of the wires.

For average lengths of 140 μm the dispersion in all matrix systems becomes increasingly difficult which is particularly apparent for the polar hybrid in Fig. 2.

For any charge transfer within the metallic network not only long range separation by the polymer matrix is critical. In addition, adjacent nanowires may be insulated by the PVP layers on their surface. It has been reported that temperatures between 150 and 200 °C are required for pure AgNW films in order to establish the best possible conductivity [35, 36]. Under these conditions, the PVP insulation is removed and a physical contact between the silver wires is established by "welding". At higher temperatures the microstructure of the nanowire is degraded due to melting and the formation of separated silver structures [35].

In Fig. 3 the conductivity of different AgNW composites are given as a function of film treatment temperature. All samples were prepared with a silver concentration of 3 vol% and an average nanowire length of 7 μm. As the conductivities were in a close range, the data were normalized to the respective maximum conductivity for better visibility.

The conductivity of all composites initially increases due to the removal of PVP from the silver surface and welding of the nanowires. A maximum conductivity is obtained after heating to 230 °C for the silicone matrix, 240 °C for the nonpolar hybrid, and 250 °C for the polar hybrid. At higher temperatures the conductivity decreases presumably due to the degradation of the nanowires.

These results reveal different facts: firstly, all matrix systems stabilize the conductive networks compared with

Fig. 2 Laser scanning microscopy images of AgNW composites using different average nanowire lengths. In total, 3 vol% of silver nanowires were incorporated in a silicone, nonpolar hybrid and polar hybrid matrix respectively
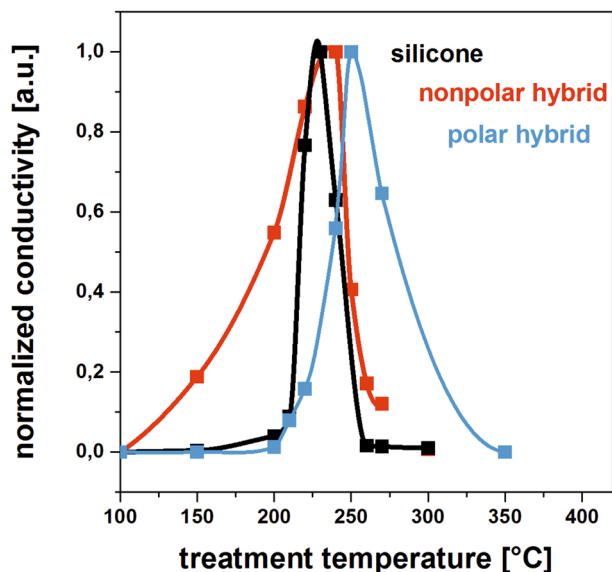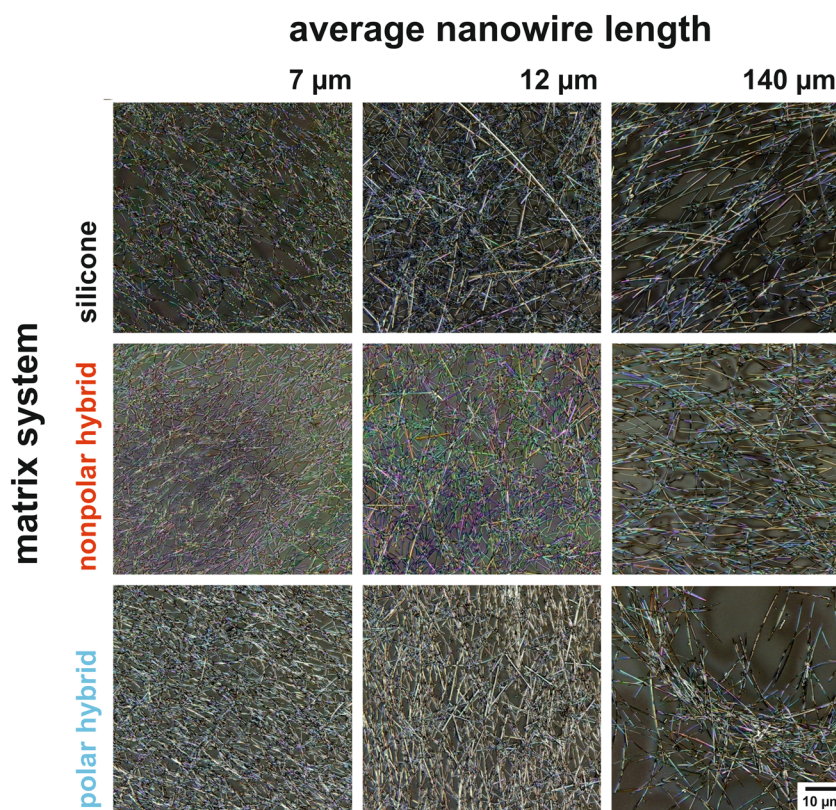

Fig. 3 Normalized conductivity of different AgNW composites as a function of film treatment temperature

pure AgNW films were the performance already starts to drop above 150–200 °C [32, 35]. This may indicate that the PVP layer adsorbed on the silver surface is protected by the matrices and the contact between the wires (as well as the subsequent nanowire degradation) is shifted to higher temperatures.

This interpretation is supported by a second observation: the temperature of maximum conductivity seems to scales with the respective matrix polarity (compare Fig. 1). As the PVP molecules are highly polar they are expected to establish better noncovalent interactions to a polar matrix, the interface is therefore stabilized.

Upon closer inspection of Fig. 3 it can be seen that the formation of an electroconductive network and its degradation proceeds in a narrow temperature range within a silicone matrix. In contrast to that the width of this thermal zone is significantly broader for both organic–inorganic hybrid systems. In these materials regions that are mainly composed of an inorganic network, coexist with zones that are dominated by organic material. The thermal processes that lead to the formation of the metallic network (and subsequently to its disintegration) are likely to depend on the local chemical environment. The inhomogeneity on the organic–inorganic hybrid matrix nanoscale therefore will broaden the relevant temperature range.

Besides these theoretical evaluations the above findings have a practical consequence: for all subsequent investigations the treatment temperature of the films was fixed to 230 °C for silicone, to 240 °C for the nonpolar, and to 250 °C for the polar hybrid matrix in order to obtain maximum conductivity for the respective AgNW composite.

The nanowire concentration as well as their average length will have a decisive effect on the electrical and
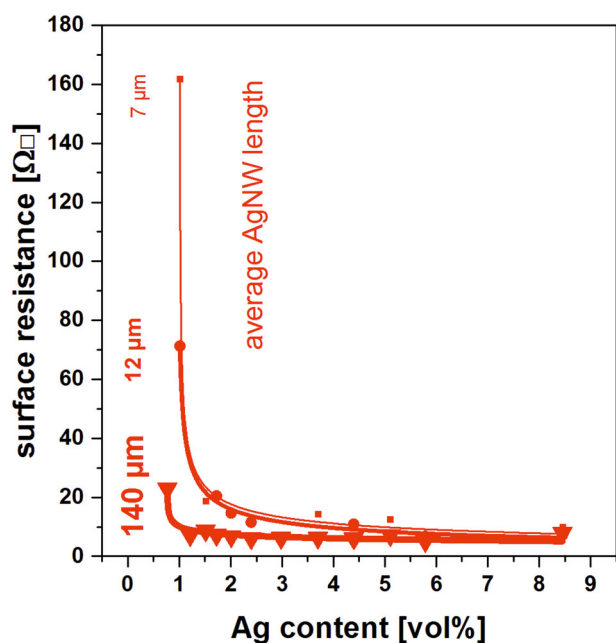
Fig. 4 Surface resistance of a nonpolar hybrid AgNW composite as a function of silver content for different average nanowire lengths

Fig. 5 Optical transmittance at 550 nm for AgNW composites with different silver contents as a function of sheet resistance

Table 1 Properties of different AgNW composite films

Matrix system	Silicone	Nonpolar hybrid	Polar hybrid
Treatment temperature [°C]	220	230	250
Film thickness [µm]	330	290	225
Sheet resistance [Ω □]	4.58	4.84	7.23
Specific resistance [Ω cm]	1.51E−04	1.40E−04	1.63E−04
Transmittance at 550 nm [%]	79	76	63
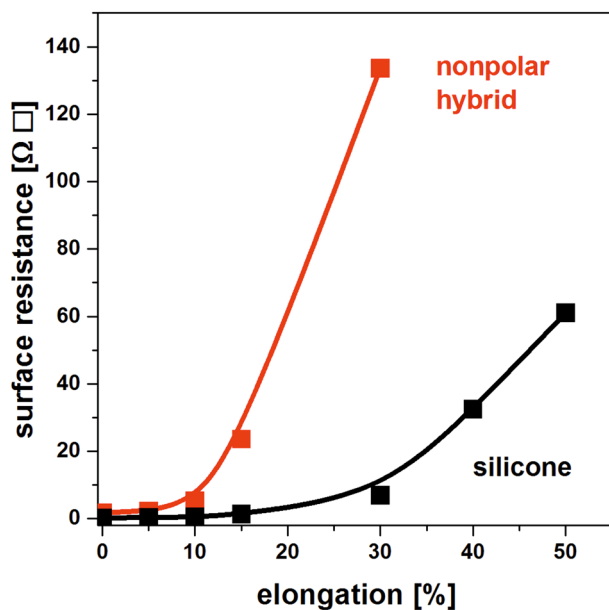
Fig. 6 Surface resistance of different AgNW composites as function of film elongation

optical performance of the composite films. As no significant difference between the different matrix systems under investigation was found, in Fig. 4 the surface conductivity of a nonpolar AgNW composite is given as an example. For silver contents exceeding 4 vol% the composites have a surface resistance of ~10 Ω □ irrespective their average length. A percolating AgNW network exists and further metallic pathways do not further increase the conductivity. At lower silver contents the resistivity slowly increases until a steep upraise indicates the disruption of material percolation. This threshold is reached at a silver concentration of 1.5 vol% for average wire lengths of 7 and 12 µm, no difference was measured between these batches. For AgNWs with an average length of 140 µm the percolation is interrupted below 1 vol%.

For practical and economic reasons we relied on lab-made silver nanowires which were regularly synthesized with average lengths between 10 and 20 µm. Occasionally larger lengths were obtained and such materials are also commercially available. Nevertheless, Fig. 4 indicates that such batches do not result in an excessive improvement of electrical performance. As stated above (Fig. 2) longer nanowires may impede their homogeneous dispersibility in the matrix systems. We therefore conclude that the use of AgNW lengths between 10 and 20 µm is reasonable, especially if a commercialization of functional composites is considered.

In order to investigate the optical properties, composites containing AgNW of an average length of 12 µm were prepared and their silver content was varied. In Fig. 5 their
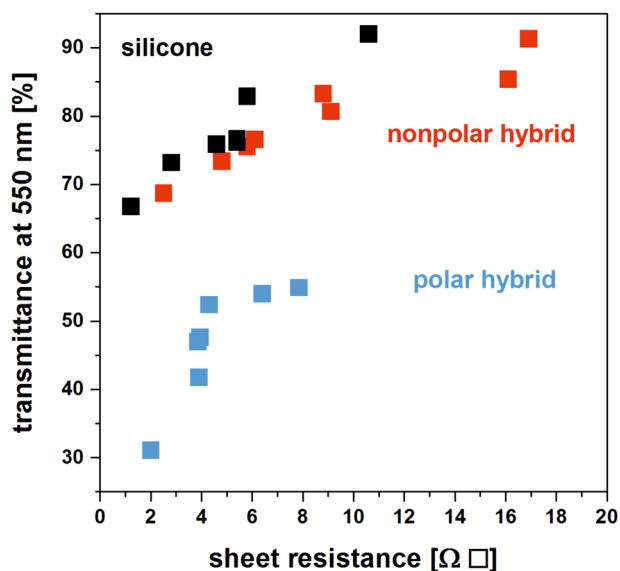
Fig. 7 Photograph (left) and LSM image (right) of a nonpolar hybrid AgNW composite film microstructured by UV lithography
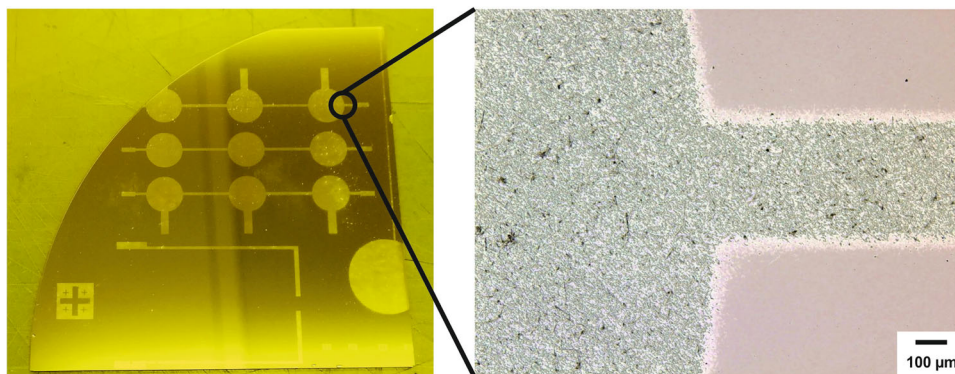
transmittance is given as a function of the resulting sheet resistance.

In general, the optical transmittance drops as the silver content is raised which causes the improvement of sheet resistance. The results are comparable if silicone and the nonpolar hybrid are used as the matrix. In contrast to that the optical transmittance is ~20% lower for the polar hybrid system. In this composition an UV initiator (Ciba® Irgacure® 369) is required which leads to slight coloration of the films and thus to the observed loss of transmittance.

For the technical evaluation of conductive films their sheet resistance often is quoted. Considering the respective thickness the specific film resistance can be calculated. In Table 1 such representative data are given along with other parameters.

The above data show excellent results regarding processing parameters and optoelectronic properties. While TCOs require high posttreatment temperatures exceeding 300 °C the silver nanowire composites can be cured and activated at lower temperatures. Furthermore, a comparison of the specific resistances ($\sim 1 \times 10^{-4}\,\Omega\,cm$) with the commonly used conductive oxides illustrates good electrical properties for technical performances and are in no way inferior to them [37].

For applications, where transparent conducting coatings have to be bended or even stretched, brittle oxide films such as ITO, AZO, and ATO cannot be used. Here composites of flexible polymers with AgNWs may offer prominent features. The polar hybrid under investigation in this study, however, had initially been developed as a scratch-resistant coating. AgNW composites based on this formulation thus may provide high mechanical strength, but their flexibility is rather limited. When such films were deposited on soft substrates, they already lost their electric conductivity under moderate mechanical wear. In contrast to that, AgNW composites based on silicone and the nonpolar hybrid exhibit a significant higher durability. In Fig. 6 the surface resistance of such films is given as a function of elongation. For both systems, the sheet

resistance remains below $10\,\Omega\,\square$ for elongations up to 10%. In the case of the nonpolar hybrid, the resistance significantly increases at higher distensions, above 30% no conductivity is measured anymore. Under these conditions cracks can be observed, obviously, the silver nanowires rupture within their matrix. In contrast to that higher electric conductivity is maintained for the silicone-AgNW composite for large elongations.

Regarding the electromechanical properties silicone outperforms the nonpolar hybrid as matrix material. In contrast to standard silicone formulations, however, the nonpolar organic–inorganic hybrid can be microstructured by UV lithography. This feature may be essential for applications where the design of transparent circuitry is required. In Fig. 7 the photograph of such a conductive path is given along with a cutout image taken by LSM at higher magnification.

As can be seen from the images the composite film is clearly separated from areas where it has been removed throughout the developing process. It is focus of ongoing research to determine the spatial resolution that can be obtained by UV lithography. In this context, it is expected that the average length of the embedded nanowires will be a decisive factor.

4 Conclusions

It is possible to homogeneously incorporate silver nanowires into organic–inorganic hybrids. Films prepared from such composites can exhibit a specific resistivity as low as $1.40E{-}04\,\Omega\,cm$ with a transparency of 76% at 550 nm. Electric conductivity is maintained throughout stretching up to 30%. As laterally structured conductive pathways can be obtained by UV lithography these AgNW composites are suitable for the fabrication of stretchable transparent electronics.

Compliance with ethical standards

References

1. Ducamp-Sanguesa C, Herrera-Urbina R, Figlarz M (1992) Synthesis and characterization of fine and monodisperse silver particles of uniform shape. J Solid State Chem 100(2):272–280

2. Xue Q, Yao W, Liu J et al. (2017) Facile synthesis of silver nanowires with different aspect ratios and used as high-performance flexible transparent electrodes. Nanoscale Res Lett 12(1):480. https://doi.org/10.1186/s11671-017-2259-6

3. Žeželj M, Stanković I, Belić A (2012) Finite-size scaling in asymmetric systems of percolating sticks. Phys Rev E Stat Nonlin Soft Matter Phys 85(2 Pt 1):21101. https://doi.org/10.1103/PhysRevE.85.021101

4. Cortes LQ, Lonjon A, Dantras E et al. (2014) High-performance thermoplastic composites poly(ether ketone ketone)/silver nanowires: morphological, mechanical and electrical properties. J Non-Cryst Solids 391:106–111. https://doi.org/10.1016/j.jnoncrysol.2014.03.016

5. Jung J, Cho H, Yuksel R et al. (2019) Stretchable/flexible silver nanowire electrodes for energy device applications. Nanoscale 11 (43):20356–20378. https://doi.org/10.1039/c9nr04193a

6. Gelves GA, Lin B, Sundararaj U et al. (2006) Low electrical percolation threshold of silver and copper nanowires in polystyrene composites. Adv Funct Mater 16(18):2423–2430. https://doi.org/10.1002/adfm.200600336

7. Hu L, Wu H, Cui Y (2011) Metal nanogrids, nanowires, and nanofibers for transparent electrodes. MRS Bull 36(10):760–765. https://doi.org/10.1557/mrs.2011.234

8. Jiu J, Nogi M, Sugahara T et al. (2012) Strongly adhesive and flexible transparent silver nanowire conductive films fabricated with a high-intensity pulsed light technique. J Mater Chem 22 (44):23561. https://doi.org/10.1039/c2jm35545k

9. Li J, Liang J, Jian X et al. (2014) A flexible and transparent thin film heater based on a silver nanowire/heat-resistant polymer composite. Macromol Mater Eng 299(11):1403–1409. https://doi.org/10.1002/mame.201400097

10. Kim Y, Lee DH, Kim D-H et al. (2015) Flexible and transparent electrode based on silver nanowires and a urethane acrylate incorporating Diels–Alder adducts. Mater Des 88:1158–1163. https://doi.org/10.1016/j.matdes.2015.09.110

11. Kim Y, Jun S, Ju B-K et al. (2017) Heterogeneous configuration of a Ag nanowire/polymer composite structure for selectively stretchable transparent electrodes. ACS Appl Mater Interfaces 9 (8):7505–7514. https://doi.org/10.1021/acsami.6b11853

12. Park M, Park J, Jeong U (2014) Design of conductive composite elastomers for stretchable electronics. Nano Today 9(2):244–260. https://doi.org/10.1016/j.nantod.2014.04.009

13. Cheng Y, Wang R, Zhai H et al. (2017) Stretchable electronic skin based on silver nanowire composite fiber electrodes for sensing pressure, proximity, and multidirectional strain. Nanoscale 9 (11):3834–3842. https://doi.org/10.1039/c7nr00121e

14. Yang M, Kim SW, Zhang S et al. (2018) Facile and highly efficient fabrication of robust Ag nanowire–elastomer composite electrodes with tailored electrical properties. J Mater Chem C 6 (27):7207–7218. https://doi.org/10.1039/C8TC01691G

15. Seo JH, Hwang I, Um H-D et al. (2017) Cold isostatic-pressured silver nanowire electrodes for flexible organic solar cells via room-temperature processes. Adv Mater 29(30). https://doi.org/10.1002/adma.201701479

16. Tokuno T, Nogi M, Karakawa M et al. (2011) Fabrication of silver nanowire transparent electrodes at room temperature. Nano Res 4(12):1215–1222. https://doi.org/10.1007/s12274-011-0172-3

17. Yu Y-Y, Ting Y-J, Chung C-L et al. (2017) Comprehensive study on chemical and hot press-treated silver nanowires for efficient polymer solar cell application. Polymers 9(11). https://doi.org/10.3390/polym9110635

18. Madaria AR, Kumar A, Zhou C (2011) Large scale, highly conductive and patterned transparent films of silver nanowires on arbitrary substrates and their application in touch screens. Nanotechnology 22(24):245201. https://doi.org/10.1088/0957-4484/22/24/245201

19. Lee P, Lee J, Lee H et al. (2012) Highly stretchable and highly conductive metal electrode by very long metal nanowire percolation network. Adv Mater 24(25):3326–3332. https://doi.org/10.1002/adma.201200359

20. Song M, Park JH, Kim CS et al. (2014) Highly flexible and transparent conducting silver nanowire/ZnO composite film for organic solar cells. Nano Res 7(9):1370–1379. https://doi.org/10.1007/s12274-014-0502-3

21. Xu F, Zhu Y (2012) Highly conductive and stretchable silver nanowire conductors. Adv Mater 24(37):5117–5122. https://doi.org/10.1002/adma.201201886

22. Kim D-H, Yu K-C, Kim Y et al. (2015) Highly stretchable and mechanically stable transparent electrode based on composite of silver nanowires and polyurethane-urea. ACS Appl Mater Interfaces 7(28):15214–15222. https://doi.org/10.1021/acsami.5b04693

23. Kim K, Kim J, Hyun BG et al. (2015) Stretchable and transparent electrodes based on in-plane structures. Nanoscale 7 (35):14577–14594. https://doi.org/10.1039/c5nr04341g

24. Seshadri I, Esquenazi GL, Borca-Tasciuc T et al. (2014) Softening in silver-nanowire-filled polydimethylsiloxane nanocomposites. Appl Phys Lett 105(1):13110. https://doi.org/10.1063/1.4884648

25. Lin S-C, Ma C-CM, Liao W-H et al. (2016) Preparation of a graphene–silver nanowire hybrid/silicone rubber composite for thermal interface materials. J Taiwan Inst Chem Eng 68:396–406. https://doi.org/10.1016/j.jtice.2016.08.009

26. Haas K-H, Rose K (2003) Hybrid inorganic/organic polymers with nanoscale building blocks: precursors, processing, properties and applications. Rev Adv Mater Sci 5(1):47–52

27. Beyer M (2013) Untersuchungen zu photovernetzbaren und biokompatiblen (hybrid-) polymeren. Dissertation, Julius-Maximilians-Universität, Würzburg

28. Steenhusen S, Burmeister F, Groß M et al. (2018) Heterogeneous microoptical structures with sub-micrometer precision.

Thin Solid Films 668:74–80. https://doi.org/10.1016/j.tsf.2018.09.013

29. Sun Y, Yin Y, Mayers BT et al. (2002) Uniform silver nanowires synthesis by reducing AgNO 3 with ethylene glycol in the presence of seeds and poly(vinyl pyrrolidone). Chem Mater 14 (11):4736–4745. https://doi.org/10.1021/cm020587b

30. Wolter H, Rose K, Egger C Silane (1990) Verfahren zu ihrer Herstellung und ihre Verwendung zur Herstellung von Polymerisaten und Polykondensaten DE 4011044 A

31. Huang G-W, Xiao H-M, Fu S-Y (2015) Wearable electronics of silver-nanowire/poly(dimethylsiloxane) nanocomposite for smart clothing. Sci Rep 5:13971. https://doi.org/10.1038/srep13971

32. Larmagnac A, Eggenberger S, Janossy H et al. (2014) Stretchable electronics based on Ag-PDMS composites. Sci Rep. 4:7254. https://doi.org/10.1038/srep07254

33. Ho X, Nie Tey J, Liu W et al. (2013) Biaxially stretchable silver nanowire transparent conductors. J Appl Phys 113(4):44311. https://doi.org/10.1063/1.4789795

34. Lee J, Lee I, Kim T-S et al. (2013) Efficient welding of silver nanowire networks without post-processing. Small 9(17):2887–2894. https://doi.org/10.1002/smll.201203142

35. Langley D, Giusti G, Mayousse C et al. (2013) Flexible transparent conductive materials based on silver nanowire networks: a review. Nanotechnology 24(45):452001. https://doi.org/10.1088/0957-4484/24/45/452001

36. Langley DP, Lagrange M, Giusti G et al. (2014) Metallic nanowire networks: effects of thermal annealing on electrical resistance. Nanoscale 6(22):13535–13543. https://doi.org/10.1039/c4nr04151h

37. Löbmann P (2013) Transparent conducting oxides. In: *Chemical solution deposition of functional oxide thin films*. Springer, pp 655–672